Sustained Increases in Lower-Tropospheric Subsidence over the Central Tropical North Pacific Drive a Decline in High-Elevation Rainfall in Hawaii

RYAN J. LONGMAN

Department of Geography, University of Hawai'i at Mānoa, Honolulu, Hawaii

HENRY F. DIAZ

NOAA/Earth System Research Laboratory, and Cooperative Institute for Research in Environmental Sciences, University of Colorado Boulder, Boulder, Colorado

THOMAS W. GIAMBELLUCA

Department of Geography, University of Hawai'i at Mānoa, Honolulu, Hawaii

(Manuscript received 29 December 2014, in final form 11 August 2015)

ABSTRACT

Consistent increases in the strength and frequency of occurrence of the trade wind inversion (TWI) are identified across a ~40-yr period (1973–2013) in Hawaii. Changepoint analysis indicates that a marked shift occurred in the early 1990s resulting in a 20% increase in the mean TWI frequency between the periods 1973–90 and 1991–2013, based on the average of changes at two sounding stations and two 6-month (dry and wet) seasons. Regional increases in the atmospheric subsidence are identified in four reanalysis datasets over the same ~40-yr time period. The post-1990 period mean for the NCEP–NCAR reanalysis shows increases in subsidence of 33% and 41% for the dry and wet seasons, respectively. Good agreement was found between the time series of TWI frequency of occurrence and omega, suggesting that previously reported increases in the intensity of Hadley cell subsidence are driving the observed increases in TWI frequency. Correlations between omega and large-scale modes of internal climate variability such as El Niño–Southern Oscillation (ENSO) and the Pacific decadal oscillation (PDO) do not explain the abrupt shift in TWI frequency in the early 1990s in both seasons. Reported increases in TWI frequency of occurrence may provide some explanation for climate change–related precipitation change at high elevations in Hawaii. On average, post-1990 rainfall was 6% lower in the dry season and 31% lower in the wet season at nine high-elevation sites. Rainfall was significantly correlated with TWI frequency at all of the stations analyzed.

1. Introduction

The effects of climate change in the Hawaiian Islands has received considerable attention in recent years (e.g., Cao et al. 2007; Giambelluca et al. 2008; Timm and Diaz 2009; Chu et al. 2010; Diaz et al. 2011; Elison Timm et al. 2011; Bassiouni and Oki 2013; Diaz and Giambelluca 2012; Krushelnycky et al. 2013; Longman et al. 2014, 2015). Increases in temperature (Giambelluca et al. 2008), decreases in precipitation, and increased drought occurrence (e.g., Chu and Chen 2005; Levinson and Kruk 2008; Diaz and Giambelluca 2012), particularly at high elevations (e.g., Krushelnycky et al. 2013; Frazier et al. 2013), have been observed in Hawaii over the past several decades. However, the driving forces behind these changes are not clearly understood. One possible explanation of decreased high-elevation rainfall is an increase in the frequency of occurrence of the trade wind inversion (TWI). The thermally driven Hadley cell (HC) circulation moves air vertically to a height of about 15 km within the intertropical convergence zone, and then poleward to the subtropics, where air descends. The TWI is a result of the HC subsidence interacting with convectively driven air rising from lower levels, which causes a discontinuity in the vertical temperature profile (Riehl 1979). When the TWI is present, the vertical development of clouds is suppressed and the

Corresponding author address: R. J. Longman, Department of Geography, University of Hawai'i at Mānoa, 2424 Maile Way, Saunders Hall 445, Honolulu, HI 96822.
E-mail: rlongman@hawaii.edu

DOI: 10.1175/JCLI-D-15-0006.1

© 2015 American Meteorological Society

transport of moisture to high-elevation ecosystems above the inversion on Hawaii's highest mountains is inhibited (Giambelluca 2005). The TWI is a prominent feature in the Hawaiian climate system occurring ~82% of the year and disruptions to the TWI are mainly associated with occurrences of midlatitude-type cyclonic disturbances, which are common during the wet season (Cao et al. 2007).

Several studies have been conducted to document the characteristics of the TWI (e.g., Riehl 1979; Giambelluca and Nullet 1991; Cao et al. 2007), and to determine the effects it has on the climate (e.g., Loope and Giambelluca 1998; Longman et al. 2015) and on ecological processes (e.g., Kitayama and Mueller-Dombois 1992; Krushelnycky et al. 2013; Crausbay et al. 2014; Gotsch et al. 2014) at high elevations in Hawaii. Cao et al. (2007) identified the TWI using data from two long-term radiosonde stations in Hawaii (Hilo and Līhu'e) and showed an increase in TWI frequency of occurrence and a decrease in base height for most months analyzed from 1979 to 2003. Whether or not these trends persisted or abated over the next decade has not been determined.

Longman et al. (2014) have shown that dry season solar radiation has significantly increased at four high-elevation (>2000 m) stations on the island of Maui, Hawaii, from ~1988 to 2013, which, at least for the period of high-resolution MODIS satellite imagery (since 2001), can be explained by a decrease in cloud cover. Examination of variations in the frequency of occurrence and base height of the TWI is relevant to understanding the causes of the observed trends in cloud cover and solar radiation at high elevations. In addition, it is important to understand the driving forces behind TWI variability including the response to changes in HC circulation and to phase changes in the internal modes of climate variability operating on interannual and/or interdecadal time scales.

A strong body of evidence now exists indicating that the tropical circulation belt has both widened and intensified over the past several decades (Lucas et al. 2014, and references therein). However, the rates of change in extent and intensity are not known with a high degree of certainty (Quan et al. 2014). In addition, opinions in the current literature differ regarding the relationship between widening and intensification. Some modeling efforts have shown an inverse relationship between HC intensity and expansion (e.g., Mitas and Clement 2006; Lu et al. 2007), while other research has found a positive relationship between these variables (Tanaka et al. 2004; Quan et al. 2004; Nguyen et al. 2013). Hadley cell variations are most commonly defined using the mass-weighted zonal mean meridional streamfunction (e.g., Oort and Yienger 1996; Trenberth et al. 2000; Quan et al. 2004; Stachnik and Schumacher 2011). However, they can also be defined in terms of velocity potential or vertical velocity (omega) at specific pressure levels (Wang 2002; Tanaka et al. 2004), the meridional component of divergent wind (Song and Zhang 2007), or variations in meridional atmospheric moisture transport (Sohn and Park 2010). Changes in HC are also assessed using proxy data such as outward longwave radiation (OLR) (e.g., Hu and Fu 2007) or sea level pressure (SLP) (e.g., Song and Zhang 2007).

Changes in HC width and intensity have been explained by multiple climate forcing mechanisms such as, increases in greenhouse gas (GHG) concentrations and associated changes in the sea surface temperature (SST; e.g., Staten et al. 2012), stratospheric ozone depletion (e.g., Polvani et al. 2011), and the effects of aerosols (e.g., Allen et al. 2012). Natural variability such as El Niño–Southern Oscillation (ENSO) and the Pacific decadal oscillation (PDO) have also been found to affect HC width and intensity (e.g., Mitas and Clement 2005; Grassi et al. 2012). During the warm (cool) phase of ENSO the HC is narrower (wider) and more (less) intense (Oort and Yienger 1996). Negative-phase PDO conditions have been shown to promote a widening of the tropical belt at least during the equinox seasons (Grassi et al. 2012).

Many of the studies that examine changes to the HC make use of one or more of eight available global reanalysis data products (Davis and Rosenlof 2012; Lucas et al. 2014). The majority of reanalysis products are limited to the satellite era with only three of the eight available reanalysis time series extending back to the presatellite era. Reanalysis data are not without their shortcomings and many differences among the datasets have been identified in the literature (e.g., Song and Zhang 2007; Stachnik and Schumacher 2011; Nguyen et al. 2013; Lucas et al. 2014). The inclusion or exclusion of satellite data and differences in the physics of the underlying models are potential sources of differences among the various reanalysis products (Lucas et al. 2014). Thorne and Vose (2010) note that because of these systematic differences it is crucial to examine a variety of reanalysis datasets to validate a climate change signal.

In this study, we analyze TWI data obtained from two atmospheric sounding stations, the vertical velocity of wind variable ''omega'' from four reanalysis products, and rainfall data from nine high-elevation climate stations. The overall goal for this study is to determine the proximal causes of TWI variability and the role that TWI variability has on high-elevation

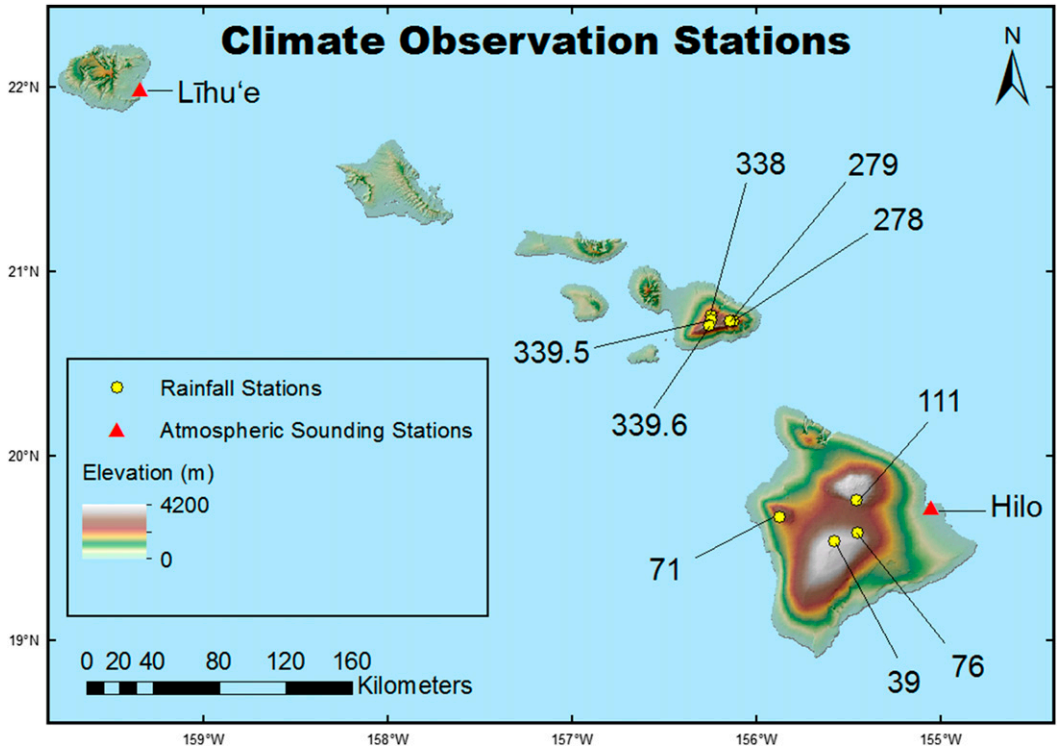

FIG. 1. Atmospheric sounding and rainfall stations used in this analysis. Rainfall stations are referenced by the state key number found in the Rainfall Atlas of Hawaii.

rainfall patterns in Hawaii. Our main objectives are to determine 1) whether previously detected increases in TWI frequency and decreases in TWI base height persisted after 2003; 2) whether changes in TWI characteristics are significantly correlated with changes in atmospheric general circulation; 3) the role of large-scale modes of internal variability, such as ENSO and PDO, in explaining TWI variability; and 4) the effects of changes in TWI frequency on rainfall regimes at high elevations, for the two 6-month seasons in Hawaii.

2. Data

We calculate TWI characteristics from vertical profiles of temperature and relative humidity obtained at two atmospheric sounding stations in Hawaii located at Līhu'e (21.97°N, 159.333°W) on the island of Kaua'i and Hilo (19.72°N, 155.05°W) on the Big Island (Fig. 1). The 1400 Hawaii-Aleutian Standard time (HST, HST + 10 = UTC) (0000 UTC) soundings from each station from 1973 to 2013 are used in this analysis to identify TWI characteristics over the period of record. (Atmospheric sounding data are maintained by the University of Wyoming and can be accessed online at http://weather.uwyo.edu/upperair/sounding.html.)

Omega, the Lagrangian tendency of air pressure, dp/dt ($\mathrm{Pa\,s^{-1}}$), is a measure of the vertical movement of air (positive values indicate subsiding air). Omega data at the 500-hPa level obtained from atmospheric reanalysis datasets are examined for a gridded domain centered over the main Hawaiian Islands. Four reanalysis datasets have been identified for this study (Table 1); they include the National Centers for Environmental Prediction–National Center for Atmospheric Research (NCEP–NCAR) 40-year reanalysis product (NNRP; Kalnay et al. 1996), the NCEP–U.S. Department of Energy (DOE) Atmospheric Model Intercomparison Project (AMIP-II) reanalysis product (NDRP; Kanamitsu et al. 2002), the 40-yr European Centre for Medium-Range Weather Forecasts (ECMWF) Re-Analysis (ERA-40; Uppala et al. 2005),

TABLE 1. Reanalysis datasets used in this analysis. Period is the range of reanalysis data used from each dataset; and spatial resolution is the latitude, longitude, and pressure levels available for each dataset.

Dataset	Source	Period	Spatial resolution
ERA-40	ECMWF	1973–2002	2.5° × 2.5° × 23
NNRP	NCEP–NCAR	1973–2013	2.5° × 2.5° × 17
NDRP	NCEP–DOE	1979–2013	2.5° × 2.5° × 17
20CR	NOAA/CIRES	1973–2012	2.0° × 2.0° × 24

and the National Oceanic and Atmospheric Administration/Cooperative Institute for Research in Environmental Sciences (NOAA/CIRES) Twentieth Century Reanalysis version 2 (20CR; Compo et al. 2011).

We chose these reanalysis datasets based on several criteria: the availability of the omega variable at 500 hPa; the period of record of available data (our analysis of TWI data begins in 1973 and, of the available reanalysis products, only NNRP, ERA-40, and 20CR include this start date), and for the spatial consistency among datasets (all four of our selected datasets are available at a horizontal resolution at either 2° × 2° (20CR) or 2.5° × 2.5° (ERA-40, NNRP, and NDRP) gridcell size; Table 1). It should be noted that the 20CR does not incorporate any upper-air or satellite observations. Omega values are averaged for a 10° × 10° grid centered over the main Hawaiian Islands (17.5°–25°N latitude, and 160°–152.5°W longitude) for 2.5° × 2.5° horizontally resolved data and 18°–24°N latitude, and 160°–152°W longitude for the 2.0° × 2.0° horizontally resolved data.

The mulitvariate ENSO index (MEI) is used to define ENSO status in this study (Wolter and Timlin 1998). The MEI incorporates six observed fields (SLP, zonal and meridional surface wind, SST, and total cloudiness) in the classification of ENSO modes. Data are obtained from NOAA (http://www.esrl.noaa.gov/psd/enso/mei/table.html). PDO index values are obtained from the Joint Institute for the Study of the Atmosphere and Ocean (JISAO) at the University of Washington (http://jisao.washington.edu/pdo/PDO.latest).

Historical rainfall data from nine high-elevation climate stations are obtained from the Rainfall Atlas of Hawaii (Giambelluca et al. 2013). We use a dataset that had been screened for outliers and inhomogeneities, and had all data gaps filled during the period 1973–2012 (Giambelluca et al. 2011). These high-elevation climate stations are located above 1900 m on the islands of Maui and Hawaii (Fig. 1).

3. Methods

a. Trade wind inversion identification

To identify TWI characteristics, sounding data were analyzed using a modification of the criteria proposed by Cao et al. (2007). The following six criteria are used to identify the TWI: 1) the TWI height is assumed to be found within the 950–650-hPa pressure range, which excludes inversions caused by radiative surface cooling below the 950-hPa level and inversions caused by the melting of cloud ice particles at altitudes above 650 hPa; 2) the TWI is identified as a layer with a positive vertical air temperature gradient and a drop in relative humidity at the same or the next (immediately higher) level; 3) apparent superadiabatic layers caused by enhanced cooling of temperature sensors emerging from the cloud zone are addressed using the method of Grindinger (1992); 4) for profiles with more than one inversion, the one with the greatest decrease in relative humidity with height is defined as the TWI layer (decreases in relative humidity are calculated as the average of the four relative humidity measurements including and immediately above the initial relative humidity drop; 5) the inversion top is identified as the bottom of the first layer above the TWI in which temperature decreases with height; and 6) inversions with a temperature change >8°C and/or thicker than 1000 m are excluded.

We characterize the TWI using three monthly interval metrics. TWI base height is identified as the mean elevation of the bottom inversion layer in each month. TWI frequency of occurrence is calculated as the number of days with an inversion present divided by the number of days of available data in each month (months with less than 75% of data are excluded from the time series). TWI strength is calculated as the mean vertical temperature gradient within the TWI layer.

b. Data aggregation and temporal assessment

Hawaii has two distinct 6-month seasons (Giambelluca and Schroeder 1998): dry (May–October) and wet (November–April). TWI and omega time series are each aggregated to a seasonal time step by averaging the six monthly values within each season. For rainfall data, the six monthly values are summed for each season. Wet seasons are identified according to the year of the beginning of the season (e.g., the wet season value for 1990 consists of data from November 1990 to April 1991). Because the TWI time series has gaps, only seasons with >75% of the data (based on the number of daily measurements available) are averaged to get a 6-month seasonal value. Most of the missing periods in the TWI time series occurred prior to 1979, and based on the minimum data criterion, we exclude the years 1975–78 from the TWI time series. After 1979 at least 92% of the data are available for all seasonal means.

An assessment of seasonal climate variability is conducted in three ways: 1) time series data are tested for trends using a linear regression model. In a preliminary analysis, 40 climate variable time series were tested for temporal autocorrelation using the Durbin–Watson statistical test (Durbin and Watson 1971). Of the 40 time series tested, 4 (10%) were significant at

TABLE 2. Seasonal TWI characteristics at Hilo and Līhu'e. Base height is the average base height of the TWI, frequency is the average frequency of occurrence of the TWI, and strength is the average strength of the TWI.

Variable	Dry season						Wet season					
	Base height (m)		Frequency (%)		Strength (°C m^{-1})		Base height (m)		Frequency (%)		Strength (°C m^{-1})	
Station	Mean	Std dev	Mean	Std dev	Mean	Std dev	Mean	Std dev	Mean	Std dev	Mean	Std dev
Hilo	2284 ±	83	80 ±	8	0.005 ±	0.001	2198 ±	89	74 ±	10	0.006 ±	0.001
Līhu'e	2131 ±	85	79 ±	12	0.004 ±	0.001	2023 ±	92	78 ±	10	0.007 ±	0.001

$\alpha = 0.05$ and 1 (4%) was significant at $\alpha = 0.01$ and no consistent patterns among stations or variables were identified. Based on these results it was decided to not include a temporal autocorrelation correction in the regression model. 2) Changepoint analysis (Killick and Eckley 2014) is used to identify significant shifts within each time series (changepoint detection is the name given to a procedure for estimating points in a time series when a statistically significant shift in the observations occurs; note: for the TWI characteristic time series, linear regression and changepoint detection is applied to the period 1979–2013, because of the 1975–78 data gap in the earlier part of the record; for the omega and rainfall data, linear regression and changepoint detection is applied using the start year of 1979. 3) We test for long-term change by comparing variable means between two different periods, delimited on the basis of the TWI changepoint results as the periods before and after the start of the 1991 dry season and referred to as P1 (1973–90) and P2 (1991–2013 for the dry season and 1991–2012 for the wet season). The difference between periods is calculated as difference = [(P1 − P2)/P1] × 100. Time series data are tested for normality using the Shapiro–Wilk statistical test (Shapiro and Wilk 1965). For datasets determined to be normally distributed, the Welch two sample t test is used to determine if there is a significant difference in the means of the two periods. Only the omega reanalysis time series were normally distributed. Some of the TWI characteristic and rainfall time series have nonnormal distributions and, therefore, the Wilcoxon rank sum test (Hollander and Wolfe 1973) is used to determine if there is a significant difference in means of the two periods. Statistical tests are conducted using R open source statistical software. We assess statistical significance at the 95% significance level ($\alpha \leq 0.05$), using the null hypothesis that the trend is zero.

In addition to the time series method described above, we also test relationships between atmospheric variables for various time periods using a linear regression method, and use the correlation coefficient (r) or the coefficient of determination (r^2) to assess the strength of the relationships between variables. Again, statistical significance is assessed at $\alpha = 0.05$.

4. Results

a. TWI characteristics and trend assessment

The TWI is a persistent high-elevation climate feature in Hawaii occurring on average 80% and 76% of the time for the dry and wet seasons, respectively (Table 2). The average dry season TWI base height is 2131 m at Līhu'e and 2284 m at Hilo. We find our results to be in close agreement with those reported by Cao et al. (2007). In a side-by-side comparison for the overlapping time period, we estimated the annual TWI frequency of occurrence to be on average 6% lower and annual TWI base height to be on average 62 m lower than those reported by Cao et al. (2007; results not shown). These differences can be explained by the modifications that were made to the Cao et al. (2007) TWI identification criteria.

Trends in the TWI characteristics derived from the linear regression model for the dry and wet seasons at each of the two sounding stations are presented based on the 1979–2013 record of the 1400 HST atmospheric sounding data (Fig. 2). For the dry season, slight decreases in base height were observed at Hilo (-0.4 m yr^{-1}) and increases were observed at Līhu'e (2.3 m yr^{-1}). For the wet season, small increases in base height were observed at Līhu'e (0.9 m yr^{-1}), and no base height trends were determined to be statistically significant in either season (Table 3). The frequency of TWI occurrence was observed to have increased over the period of record at both stations during both seasons. Statistically significant increases of 0.3% and 0.8% yr^{-1} (at Hilo and Līhu'e, respectively) during the dry season and 0.3% (not significant; $p = 0.056$) and 0.6% yr^{-1} (significant) during the wet season were observed. Increases in TWI frequency were greater at Līhu'e, which is located ~2° north of the Hilo station. Significant increases in TWI strength were observed at both stations in both seasons.

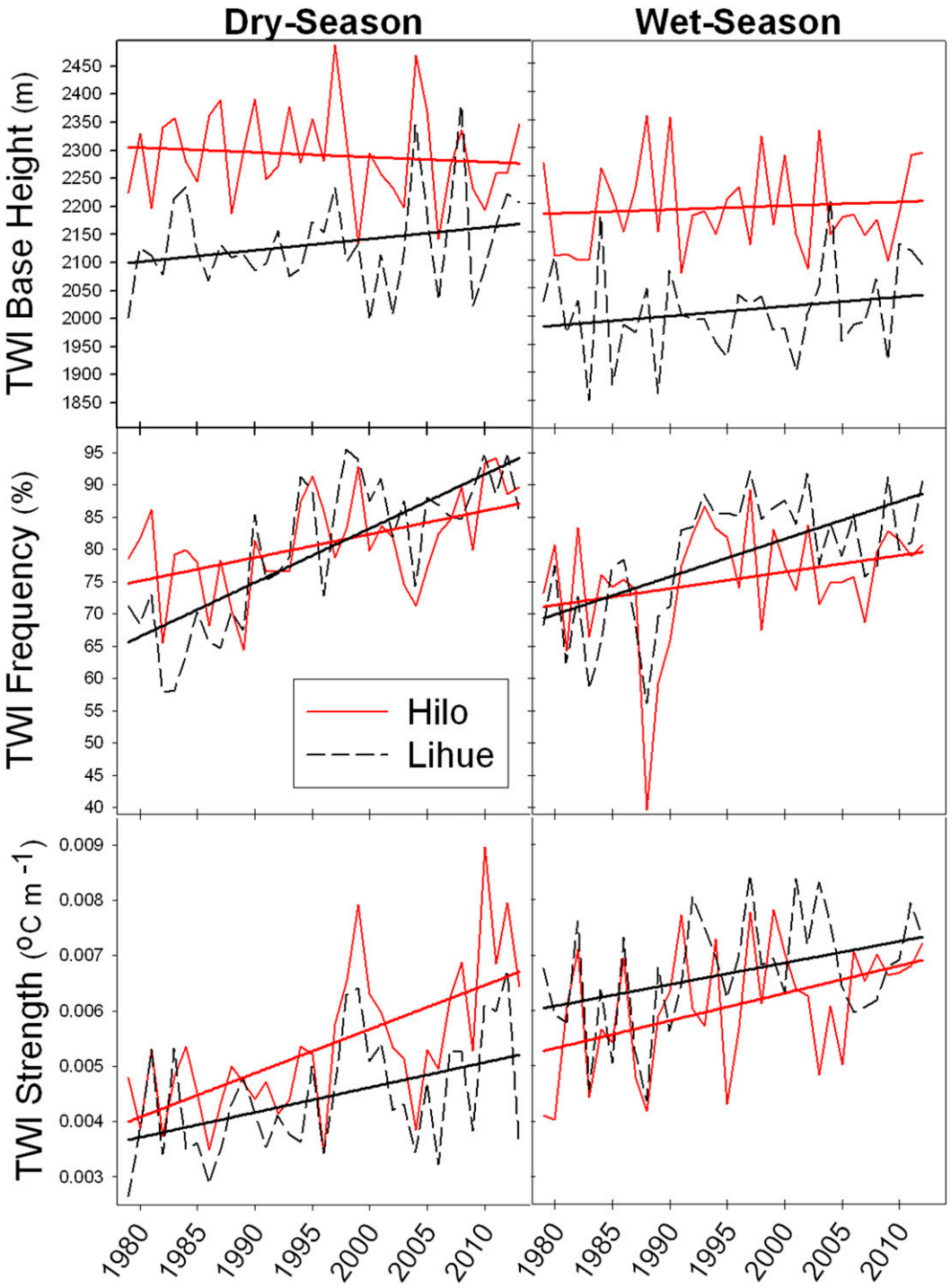

FIG. 2. TWI characteristics: (top) base height, (middle) frequency of occurrence, and (bottom) strength for (left) dry and (right) wet seasons during 1979–2013.

We applied a changepoint detection algorithm to all of the TWI time series (1979–2013) to identify any significant change years. All of the changepoint years identified mark an upward shift in TWI frequency time series. For the dry season, a TWI frequency changepoint was identified at year 1993 (Hilo) and year 1989 (Līhu'e). For the wet season, 1990 was identified as the changepoint year for both stations (Table 3). Interestingly, the year 1990 also corresponds with the start of a significant decline of an endemic plant species found

TABLE 3. Least squares regression results for TWI variables (1979–2013). Trend is the slope of the regression line, r^2 is the coefficient of determination, standard error (SE) is the standard error of the slope in the same units as trend for each variable, p is a measure of statistical significance (p values <0.05 are shown in boldface), and "C-Y" is the year at which a statistically significant shift in the data occurs. For the dry season $n = 34$; for the wet season $n = 33$.

	Dry season					Wet season				
		r^2	SE	p	C-Y		r^2	SE	p	C-Y
Base height	Trend (m yr^{-1})					Trend (m yr^{-1})				
Hilo	−0.4	0.00	1.34	0.767	No	0.0	0.00	1.40	0.991	No
Līhu'e	2.3	0.08	1.35	0.093	2003	0.9	0.01	1.43	0.523	No
Frequency	Trend (% yr^{-1})					Trend (% yr^{-1})				
Hilo	0.34	0.24	0.11	**0.003**	1993	0.30	0.11	0.15	0.056	1990
Līhu'e	0.79	0.58	0.11	**0.000**	1989	0.58	0.40	0.13	**0.000**	1990
Strength	Trend (°C m^{-1} yr^{-1})					Trend (°C m^{-1} yr^{-1})				
Hilo	0.00008	0.39	2×10^{-5}	**0.000**	No	0.00005	0.18	2×10^{-5}	**0.011**	No
Līhu'e	0.00004	0.16	2×10^{-5}	**0.016**	No	0.00004	0.13	2×10^{-5}	**0.031**	No

at high elevations on Maui, Hawaii (Krushelnycky et al. 2013). Based on these results and in an effort to maintain consistency throughout this analysis, the year 1990 is chosen as the changepoint for our time period comparison. TWI frequency data are separated into periods that correspond to observations occurring before (P1) and after (P2) the 1990 changepoint. For the dry season, P2 means were higher for; TWI base height (0.1% and 1.2% for Hilo and Līhu'e, respectively; not significant), frequency of occurrence (11% and 29%; significant at both stations), and strength (19% and 16%; significant at Hilo) (Table 4). For the wet season, P2 means were found to be lower for TWI base height (−0.6% and −0.5%; not significant), and higher for TWI frequency of occurrence (16% and 24%; significant at both stations) and strength (22% and 24%; significant at both stations). TWI frequency of occurrence was significantly higher during P2 than P1 at both stations for both wet and dry seasons (Fig. 3).

b. *Omega trend assessment*

Gridded data obtained from four reanalysis products for the variable omega at the 500-hPa level are each averaged for a 10° × 10° field centered over the Hawaiian Islands. Regression analysis indicates a consistent increase in omega (enhanced subsidence) for both the dry and wet seasons for all reanalysis products (Fig. 4). For the dry season, increases in omega range from 0.0001 to 0.0005 hPa s^{-1} yr^{-1} and were determined to be statistically significant for two of the four reanalysis products (Table 5). For the wet season, increases ranged from 0.000 02 to 0.0007 hPa s^{-1} yr^{-1} and only the ERA-40 trend was statistically significant.

Changepoint analysis applied to all of the omega time series did not reveal any significant shifts in the record. To maintain consistency, we use the year 1990 as the year for the time period comparison. Omega was found to be higher during P2 than P1 for all of the reanalysis time series for both the dry (14%–47% higher) and wet (11%–80% higher) seasons (Fig. 5 and Table 6).

To compare reanalysis products, we calculated the correlation coefficient (r) for each pair of omega time series during the time window common to all products (1979–2002; not shown). In general correlation was good among the reanalysis products ($r = 0.61$–0.94). All of the time series show stronger correlation in the wet season than the dry season. The relationship between omega and TWI frequency of occurrence (calculated as the average of Hilo and Līhu'e TWI data) is assessed using all of the available data. Significant positive correlations are found between TWI frequency of occurrence data

TABLE 4. Relative differences in TWI characteristics between time periods P1 (1973–90) and P2 (1991–2013). Diff is the percent difference between the two time periods calculated as Diff = [(P2 mean–P1)/P1 mean] × 100 (p values <0.05 are shown in boldface).

	Dry season		Wet season	
	Diff (%)	p	Diff (%)	p
Base height				
Hilo	0.1	0.988	−0.6	0.860
Līhu'e	1.2	0.467	−0.5	0.835
Frequency				
Hilo	10.5	**0.005**	16.3	**0.001**
Līhu'e	28.8	**0.000**	23.8	**0.000**
Strength				
Hilo	18.8	**0.033**	23.4	**0.002**
Līhu'e	15.1	0.130	25.0	**0.000**

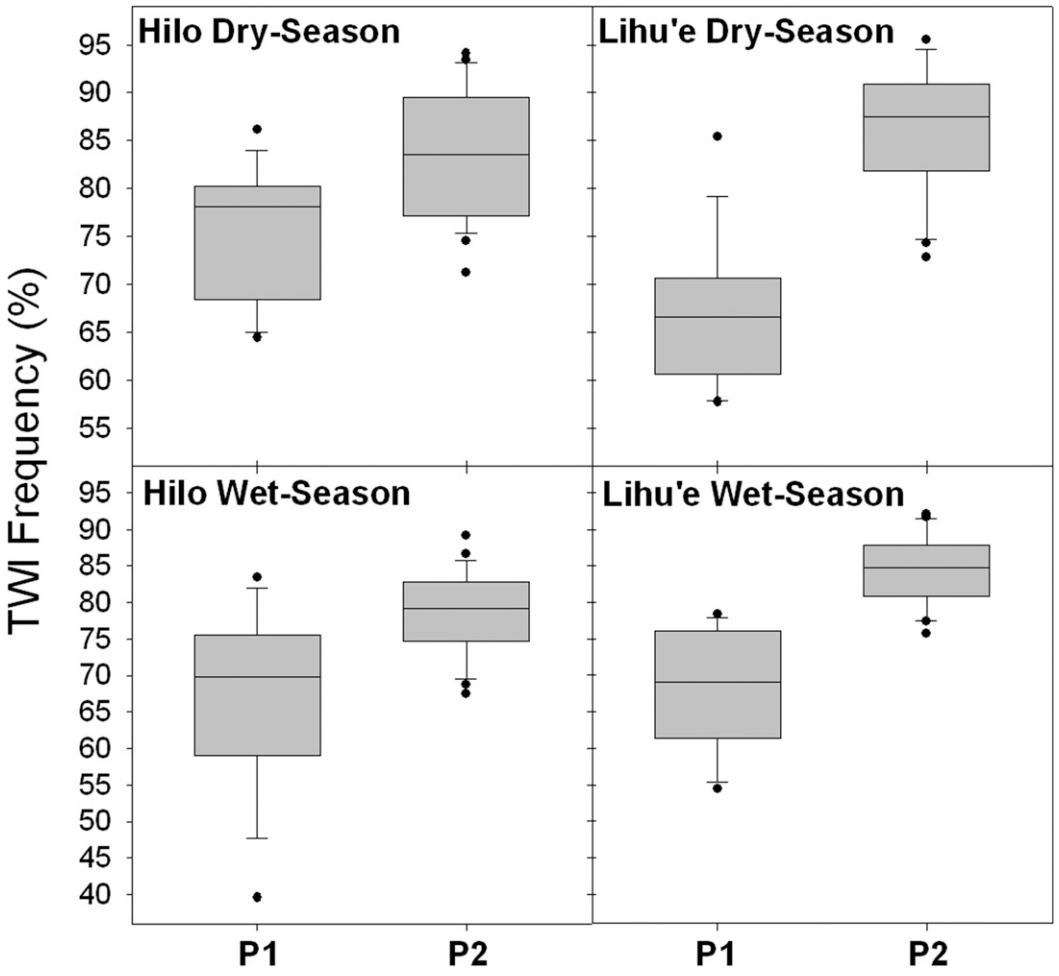

FIG. 3. TWI frequency of occurrence for (left) Hilo and (right) Līhu'e for the (top) dry and (bottom) wet seasons; P1 = 1973–90; P2 = 1991–2013; the center line in the box is the median; hinge lines represent the first and third quartile; horizontal lines on the top of the whiskers refer to the maxim and minimum values excluding outliers; outliners are defined as any point >1 or >1.5 times the interquartile range (IQR).

and all of the omega time series both dry and wet seasons (Table 7).

Using the NNRP data we examine the omega field in each season for the Northern Hemisphere (0°–50°N latitude). Clear evidence of higher P2 subsidence in both the dry and wet seasons is rather widespread along the latitude belt where the Hawaiian Islands are located (Fig. 6). The widespread intensification of atmospheric subsidence shown here may be explained by an intensification of the HC, which has been previously identified by others (e.g., Lucas et al. 2014).

c. *ENSO and PDO assessment*

All TWI frequency and omega data available between 1973 and 2013 were tested against the MEI and PDO indices. In general, correlations of TWI frequency or omega with either MEI or PDO had opposite signs for dry and wet seasons (Fig. 7). Linear regression results indicate no significant correlation between the MEI and TWI frequency ($r = -0.17$) or omega derived from the four reanalysis products ($r = -0.23$ to 0.24) during the dry season (Table 7). Wet season correlations are slightly stronger for TWI frequency ($r = 0.41$; significant) and omega ($r = 0.26$–0.47; significant for the ERA-40, NNRP, and 20CR omega time series). Data are also compared with the PDO index. During the dry season, PDO is significantly correlated with TWI frequency ($r = -0.48$) and NNRP omega ($r = -0.33$) but not significantly correlated with the three remaining reanalysis products ($r = -0.02$ to -0.27). For the wet season, no significant correlation was found between PDO and TWI frequency ($r = 0.24$) and correlations between PDO and omega were positive but weak for three of the four comparisons

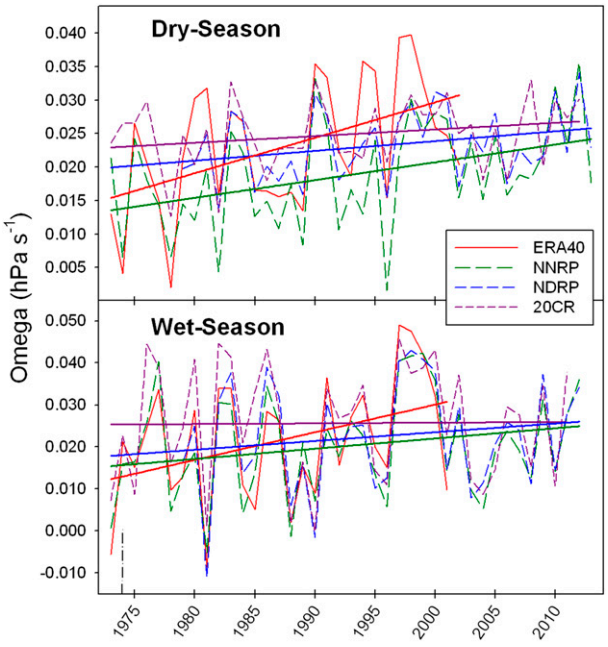

FIG. 4. Average omega from four reanalysis products for (top) dry and (bottom) wet seasons.

(r = 0.24–0.50; significant for the 20CR omega time series).

Despite weak correlations, ENSO and PDO clearly have some effect on the variability of TWI frequency especially in the wet season, for which significant relationships were identified between the MEI index and both the TWI frequency and three of the four omega time series. For the dry season, a significant relationship was found between the PDO and both the TWI frequency and NNRP omega time series. This is not surprising considering that the PDO has been shown to have a more dominant effect on climate in the dry season (see Frazier et al. 2012). It is also important to note that the relationships between these variables have opposite signs in the dry and wet seasons (Fig. 7). Considering this, phase changes to these Pacific centered modes do not explain the long-term increase (or shift) in TWI frequency reported earlier, which were consistently found in both seasons (Table 3). In general, correlations between TWI frequency and both the MEI and PDO indices are improved when time series are compared for the shorter P1 and P2 time periods and not assessed for the complete period of record.

d. Rainfall trend assessment

We calculated linear trends for the dry and wet season rainfall at nine high-elevation climate stations in Hawaii from 1973 to 2012. For the dry season, eight of the nine stations showed decreases in rainfall (−1 to −22.7 mm yr^{-1}) over the period and two of these decreases were statistically significant (Table 8). For the wet season, all nine stations showed decreases in rainfall (−3.8 to −22.2 mm yr^{-1}), three of which were statistically significant.

Changepoint detection analysis is applied to the nine rainfall time series. Results varied widely among stations and between seasons (Table 8). Because of the high variability of rainfall from year to year, the changepoint software identifies multiple changepoints in the time series. For this analysis we have constrained the software to identify the most prominent changepoint in the time series. For the dry season the most common changepoint year was 2006 (n = 4), which corresponds to a transition year from El Niño to La Niña conditions in 2007. La Niña conditions have been shown to produce predominantly below-normal precipitation conditions in the 6-month dry season (Frazier et al. 2012). For the wet season, the most common changepoint year identified was 1990 (n = 4). The year 1990 is also the year in which the significant shift in wet season TWI frequency was identified (Table 3).

Rainfall was assessed using the time period comparison defined earlier. Again, to maintain consistency among time series, we use the end of 1990 as the changepoint year (P1 = 1973–90; P2 = 1991–2012). For the dry season, results varied with lower P2 rainfall (−6% to −30%; relative to P1 rainfall) found at five stations and higher P2 rainfall (1%–5%; relative to P1 rainfall) found at the other four stations (Table 9). For the wet season, lower P2 rainfall

TABLE 5. Least squares regression results for omega (p values <0.05 are shown in boldface). Note: Time series lengths differ for each dataset ERA-40: 1973–2002, NNRP: 1973–2013, NDRP: 1979–2013, and 20CR: 1973–2012.

	Dry season						Wet season					
Dataset	Trend (hPa s^{-1} yr^{-1})	n	r^2	SE	p	C-Y	Trend (hPa s^{-1} yr^{-1})	n	r^2	SE	p	C-Y
ERA-40	0.00053	30	0.23	$2. \times 10^{-4}$	**0.008**	No	0.00066	29	0.15	$3. \times 10^{-4}$	**0.040**	No
NNRP	0.00027	41	0.16	$1. \times 10^{-4}$	**0.009**	No	0.00024	40	0.05	$2. \times 10^{-4}$	0.155	No
NDRP	0.00015	35	0.08	$9. \times 10^{-5}$	0.098	No	0.00021	34	0.03	$2. \times 10^{-4}$	0.364	No
20CR	0.00010	40	0.05	$7. \times 10^{-5}$	0.146	No	0.00002	39	0.00	$2. \times 10^{-4}$	0.935	No

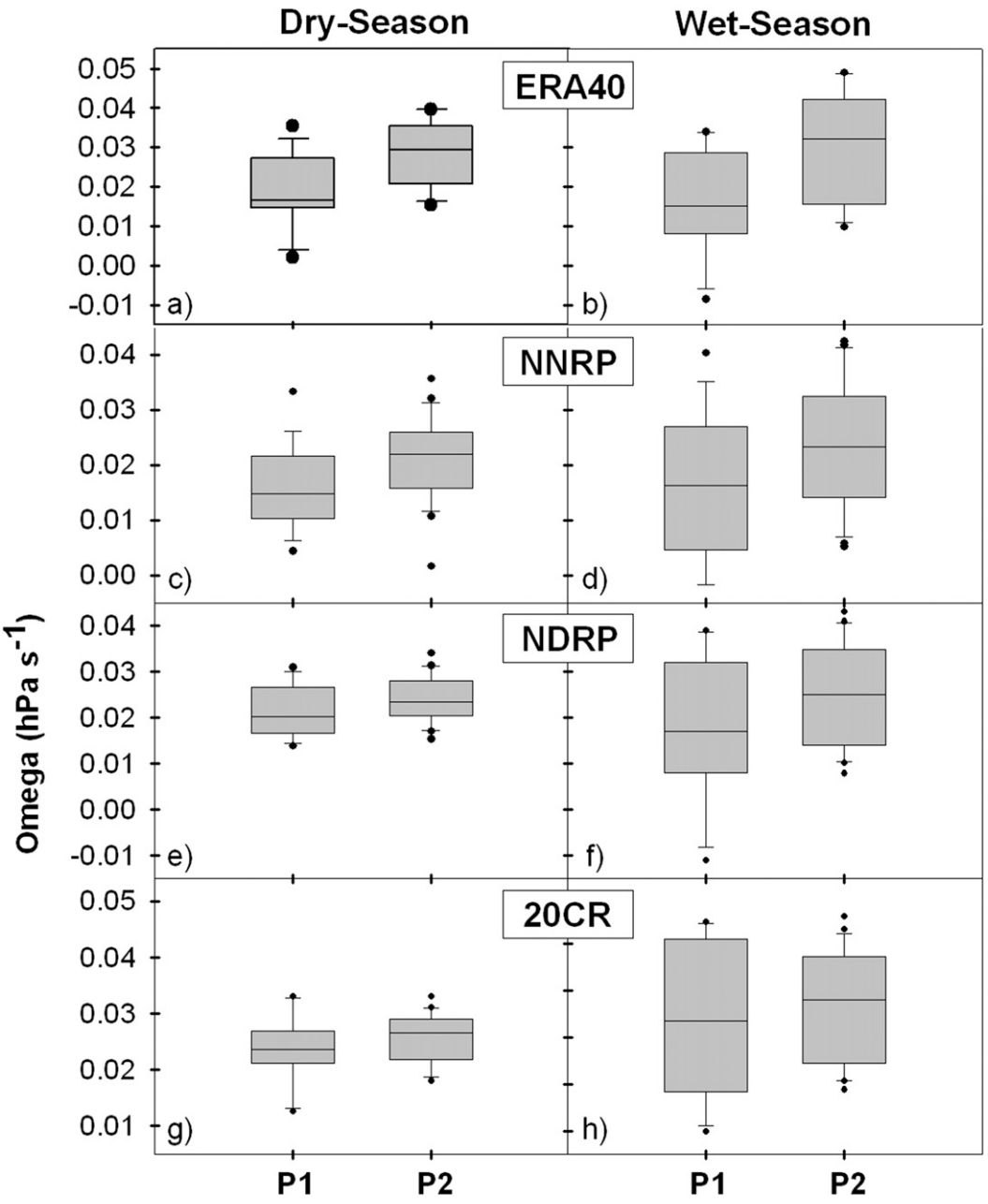

FIG. 5. Omega time period assessment results for (a),(b) ERA-40; (c),(d) NNRP; (e),(f) NDRP; and (g),(h) 20CR reanalysis products for the (left) dry and (right) wet seasons; the center line in the box is the median; hinge lines represent the first and third quartile; horizontal lines on the top of the whiskers refer to the maxim and minimum values excluding outliers; outliners are defined as any point >1 or >1.5 times the interquartile range (IQR).

(−3% to −45%; relative to P1) were found consistently at all nine stations. Seven of the nine wet season rainfall comparisons showed statistically significant increases in P2 rainfall. In general the magnitude of changes in rainfall was much greater in the wet season (Fig. 8).

We test correlations between rainfall at the nine climate stations with average TWI frequency and the NNRP-derived omega time series. Rainfall was significantly correlated with both TWI frequency and omega at all nine stations for both the dry and wet seasons (Fig. 9). This result confirms our hypothesis that increases in atmospheric subsidence and subsequent increases in TWI frequency at least partly explain the decreases in rainfall identified here. These findings also provide a physical mechanism to explain decrease

TABLE 6. Differences in mean omega between time periods P1 (1973–90) and P2 (1991–2013) (p values <0.05 are shown in boldface). Note: Time series lengths differ for each dataset ERA-40: 1973–2002, NNRP: 1973–2013, NDRP: 1979–2013, and 20CR: 1973–2012.

	Dry season		Wet season	
Dataset	Diff (%)	p	Diff (%)	p
ERA-40	47	**0.009**	80	**0.017**
NNRP	33	**0.035**	41	0.094
NDRP	14	0.133	34	0.235
20CR	47	0.216	11	0.554

in rainfall identified by others (e.g., Frazier et al. 2013, 2015).

5. Summary and discussion

Using TWI data from two atmospheric sounding stations, omega data from four reanalysis products, and rainfall data from nine high-elevation climate stations, we examined long-term changes in atmospheric subsidence over the Hawaii region and the subsequent effects that these changes have had on rainfall at high elevations.

We have found a significant increase in TWI frequency and TWI strength over the past approximately four decades for both the dry and wet seasons most notably defined by an abrupt upward shift in the early 1990s. Increases in atmospheric subsidence have been identified in four reanalysis datasets and are in agreement with changes in the TWI frequency. Considering that TWI frequency is significantly correlated with omega, we hypothesize that the increases in TWI frequency found here may be directly related to the intensification of HC subsidence that has previously been reported in the literature (see. Lucas et al. 2014).

Determining the causes of increases in HC subsidence is not within the scope of this study. However, many modeling studies have suggested multiple climate forcings that could alter the width and intensity of the HC (see Lucas et al. 2014). A primary source of tropical climate variability is ENSO, but the influence of ENSO on the HC is still debated. Oort and Yienger (1996) showed that HC intensity has a tendency to increase during the warm phase of ENSO due to enhanced convection in the equatorial central Pacific resulting in more persistent subsidence in the subtropics during the winter [December–February (DJF)] months. Quan et al. (2004) showed that HC responses to ENSO were much stronger during the warm (El Niño) phase than during the cool La Niña phase. More recently, Stachnik and Schumacher (2011) found that various reanalysis datasets show a weak, but statistically significant increase in HC intensity in the Northern Hemisphere (NH) during El Niño. In contrast to these findings, Tanaka et al. (2004) and Mitas and Clement (2005) found little relationship between the NH wintertime HC intensity and ENSO, and Caballero (2007) found that more than 70% of HC variability was not related to ENSO. To our knowledge no study has attempted to connect fluctuations in HC intensity with changes in PDO phase. However, the HC has been shown to widen during the cool phase of PDO (Grassi et al. 2012).

In this present analysis we find that correlations between TWI frequency and omega and the ENSO and PDO indices are weak and not consistent for the dry and wet seasons (Table 7). In addition, the effects these Pacific-centered modes have on TWI frequency and omega were opposite for the dry and wet seasons (Fig. 7) and are not in agreement with the approximate 1991 positive shift in TWI frequency (Fig. 3) and omega

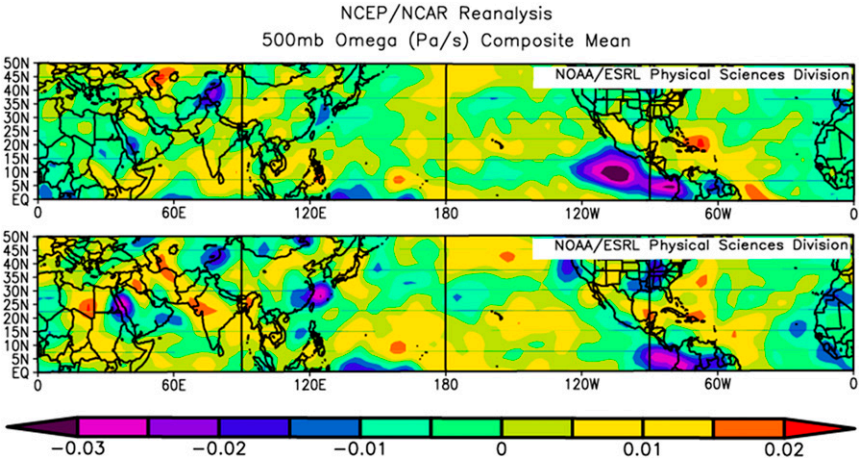

FIG. 6. Composite mean NNRP-derived omega at the 500-hPa level (differences between P1 and P2 calculated as P2 mean minus P1 mean) for (top) dry and (bottom) wet.

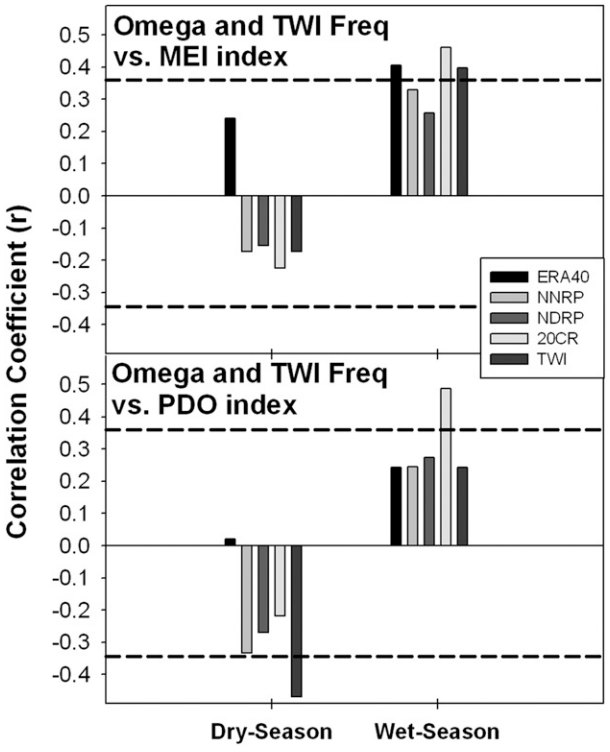

FIG. 7. Correlation coefficient (r) values derived from linear regression for omega and TWI frequency when compared with the (top) MEI index and (bottom) the PDO index for all available data in each time series; the dashed line represents the critical values of the two-sided correlation coefficient r at $\alpha = 0.05$ for $df = 32$.

TABLE 7. Correlation coefficient (r) values derived from linear regression between omega and TWI frequency and the relationship between these variables and the MEI and PDO indices for all available data from 1973 to 2013. TWI is trade wind inversion frequency of occurrence, MEI is the multivariate ENSO index, PDO is the Pacific decadal oscillation index. Note: The length of the time series are different for each variable and comparisons between variables are made using all of the available data between 1973 and 2013 (p values <0.05 are shown in boldface).

	Dry season		Wet season	
	r	p	r	p
vs TWI				
ERA-40	0.732	**0.000**	0.630	**0.001**
NNRP	0.602	**0.000**	0.580	**0.000**
NDRP	0.512	**0.002**	0.471	**0.005**
20CR	0.483	**0.003**	0.521	**0.001**
vs MEI				
ERA-40	0.240	0.202	0.407	**0.029**
NNRP	−0.173	0.280	0.330	**0.037**
NDRP	−0.155	0.375	0.256	0.143
20CR	−0.225	0.163	0.461	**0.003**
TWI	−0.179	0.289	0.410	**0.013**
vs PDO				
ERA-40	0.020	0.840	0.243	0.148
NNRP	−0.333	**0.033**	0.245	0.127
NDRP	−0.269	0.119	0.274	0.118
20CR	−0.219	0.175	0.489	**0.002**
TWI	−0.475	**0.003**	0.235	0.168

(Fig. 5) identified over the Hawaii region in this study, which occurs in both seasons. Longman (2015) demonstrated that for the wet season the warm (cool) phase of ENSO or PDO corresponds to a more (less) frequent TWI, resulting in drier (wetter) conditions at high elevations. For the dry season, these relationships are opposite (e.g., warm phase: less frequent TWI and wetter). We agree that ENSO phase changes may play some role in the variability of TWI frequency of occurrence, but statistical correlations only explain a small portion of the variance and the relationship is opposite for the two seasons (Fig. 8). The relationship between wet season TWI frequency and ENSO phase change is statistically significant, but explains only about 17% of the variance in the time series (Table 7). When subsets of the period of record (P1 and P2, before and after the end of 1990, respectively) are assessed, correlations between TWI frequencies and the MEI index are greatly improved for both seasons. When these shorter time periods are assessed, ENSO phase change explains 41% (P1) and 26% (P2) of the variance in the wet season TWI frequency time series. In general, correlations with the PDO and TWI frequency are also improved when data are separated into pre- and postshift periods. This body of evidence suggests that while both ENSO and PDO may explain some of the variability in TWI frequency they do not explain the longer-term change (i.e., the shift between the 1973–90 and 1991–2013 periods) reported here. Correlations between omega and the ENSO and PDO indices were weak and significant only in the wet season (Table 7), which suggests that alternative forcing mechanisms are potentially driving the observed increase in HC intensity. In addition to the results reported here, Merrifield (2011) has shown that a 20% increase in the amplitude of Pacific trade winds from 1990 to 2009 relative to the previous 40-yr period is linked to an increase in atmospheric circulation and is not explained by ENSO and PDO phase changes. The fact that this reorganization of the wind system is not consistent with a Pacific-only SST driving mechanism, suggests that changes outside the tropical Pacific might be important (McGregor et al. 2014). McGregor et al. (2014) has concluded that the unprecedented acceleration of the Pacific trade wind system since the early 1990s is, in fact, driven by rapid warming of the Atlantic in relation to the Pacific. The Atlantic Ocean has been shown to play an important role in low-frequency variability in the tropical Pacific via an atmospheric trans-basin coupling (Chikamoto et al. 2015). Yu et al. (2015)

TABLE 8. Time trends, based on least squares linear regression, for nine high-elevation rainfall time series (1973–2012). SKN is the state key number used to identify rainfall stations; $n = 39$ for the dry season; $n = 38$ for the wet season (p values <0.05 are shown in boldface).

		Dry season					Wet season				
SKN	Elev (m)	Trend (mm yr^{-1})	r^2	SE	p	C-Y	Trend (mm yr^{-1})	r^2	SE	p	C-Y
71	1905	−7.1	0.29	1.8	**0.000**	1997	−3.8	0.04	3.2	0.249	1996
338	2143	0.3	0.00	1.9	0.860	1976	−15.6	0.06	7.73	0.051	1990
278	2195	−22.7	0.13	9.7	**0.025**	2007	−22.2	0.00	15	0.148	1990
279	2459	−3.9	0.02	4.1	0.359	2006	−2.7	0.00	8.21	0.748	1977
76	2530	−2.8	0.06	1.9	0.141	1997	−9.9	0.18	3.47	**0.007**	1990
339.5	2589	−1.0	0.01	1.6	0.536	2006	−10.9	0.09	5.74	0.067	1990
111	2810	−2.2	0.03	1.9	0.253	2006	−11.8	0.15	4.6	**0.014**	1975
339.6	2989	−1.0	0.01	1.7	0.541	2006	−11.6	0.06	7.57	0.133	1996
39	3397	−1.6	0.04	1.3	0.211	2004	−6.4	0.11	3.01	**0.041**	1981

has suggested that a positive phase change in the Atlantic multidecadal oscillation (AMO) occurring in the early 1990s is responsible for a strengthening of the subtropical high in the Pacific and the subsequent increases in trade wind strength. The variability in coupled atmosphere–ocean modes in the Atlantic has been shown to feed back to the Pacific through a transbasin interaction and a global displacement of the Walker circulation (Chikamoto et al. 2015).

Climate forcing mechanisms unrelated to ENSO or PDO that may explain increased HC subsidence include warming due to enhanced GHG concentrations and associated SST increases, the indirect or direct effects of aerosols, and/or the depletion of stratospheric ozone, which have been hypothesized to affect HC width (Lucas et al. 2014 and references therein). Global simulations of future climate show that the margins of Hadley cell circulation will move poleward in both hemispheres and in all seasons as a result of global warming (e.g., Kang and Lu 2012). Perhaps, the increased frequency in TWI occurrence is explained by a decrease in atmospheric disturbances in the central North Pacific. Cao et al. (2007) suggested that a global warming–related poleward shift in midlatitude storm tracks (Yin 2005) would cause fewer interruptions of Hadley cell subsidence over Hawaii, thus increasing TWI persistence. The effects of this, however, would be predominantly seen in the wet season when storms are more prevalent so this does not explain the observed upward shift in TWI frequency identified in both seasons. In general, an expansion or intensification of the HC due to climate change (Seidel et al. 2008) would make interruptions of subsidence less frequent in Hawaii for both the dry and wet seasons.

To identify the effects that increases in subsidence have on seasonal high-elevation rainfall patterns we compared nine rainfall time series with TWI frequency and omega data. Our results indicate a mixed signal in the dry season and a consistent drying signal in the wet season. For the dry season, rainfall at nine stations (Fig. 8) was significantly correlated with both TWI frequency and omega. Lower P2 rainfall was identified at five stations (−6% to −31%) and higher P2 rainfall was identified at the remaining four stations (1%–5%). On average, rainfall was 6% lower during P2 relative to P1 (Table 9). These findings suggest that, in general, an increase in subsidence has contributed to a slight overall P2 decrease in high-elevation dry season rainfall although decreases at some individual stations are much more pronounced. It is not clear why some stations showed small increases in P2 rainfall despite an increase in TWI frequency. For the wet season, rainfall at all of the nine stations was significantly correlated with both TWI frequency and omega (Fig. 9) and the average P2 rainfall for the nine stations analyzed was 31% lower relative to the P1 mean (Table 9). Based on the NNRP-derived omega, the P1 to P2 increase in subsidence was 8% stronger in the wet season than the dry season. Also, the Hilo radiosonde data showed that P1 to P2 increase in TWI frequency was 6% greater during the wet season than the dry season. These results are consistent with the changes in rainfall being more pronounced in the wet season.

TABLE 9. Differences in mean rainfall between time periods P1 (1973–90) and P2 (1991–2013) (p values <0.05 are shown in boldface).

		Dry season		Wet season	
SKN	Elev (m)	Diff (%)	p	Diff (%)	p
71	1905	−30	**0.004**	−22	0.084
338	2143	5	0.778	−38	**0.022**
278	2195	−10	0.180	−21	**0.042**
279	2459	1	0.459	−3	0.798
76	2530	−9	0.240	−36	**0.015**
339.5	2589	2	0.798	−38	**0.005**
111	2810	−6	0.563	−39	**0.032**
339.6	2989	4	0.396	−32	**0.032**
39	3397	−11	0.271	−45	**0.026**

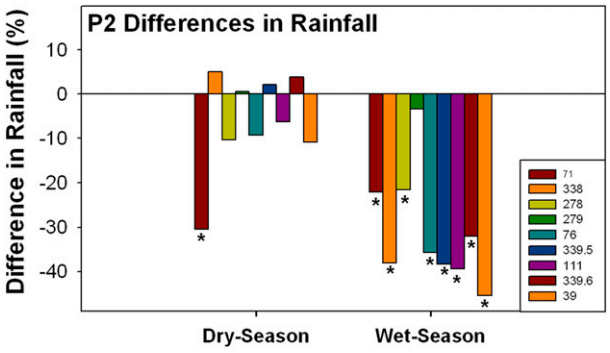

FIG. 8. Change in rainfall between 1973–90 (P1) and 1991–2012 (P2) calculated as the difference = [(P1 rainfall − P2 rainfall)/P1 rainfall] × 100. Note: Stations are positioned in order of increasing elevation (left to right) for each season; stations with an asterisk at the end of the bar indicate a statistically significant (α = 0.05) change.

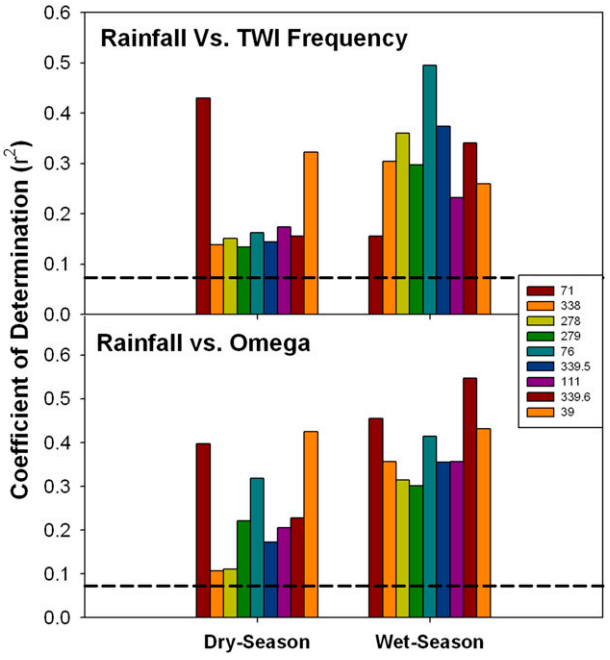

FIG. 9. Amount of variance in seasonal rainfall at nine individual stations explained by variations in two station seasonal mean (top) TWI frequency and (bottom) the NNRP omega for wet and dry seasons (1973–2012); the dashed line represents the critical values of the two sided coefficient of determination r^2 at α = 0.05 (df = 36). Note: Stations are positioned in order of increasing elevation (left to right) for each season.

The spatial dynamics and temporal trends in rainfall have been a topic of great interest to many researchers in Hawaii. Previous studies have examined rainfall variability on seasonal (Lyons 1982; Chu 1989; Frazier et al. 2013), interannual, and decadal time scales (Chu and Chen 2005; Timm and Diaz 2009, Chu et al. 2010;Elison Timm et al. 2011; Diaz and Giambelluca 2012; Frazier et al. 2013). Levinson and Kruk (2008) detected a statistically significant downward trend in rainfall since 1905 (see also Diaz and Giambelluca 2012), and Elison Timm et al. (2011) and Chu et al. (2010) have shown a decrease in the frequency of moderate and extreme rainfall events. Prior research has identified links between climate variations and the behavior of the TWI (Tran 1995) and the results from this study make a clear connection between increased TWI frequency and decreases in high-elevation rainfall in Hawaii. This is an important finding because while many authors have identified changes in rainfall over time the proximal cause behind these changes are not always clear.

In other studies, Diaz et al. (2011) found evidence of drying in vertical humidity profiles at higher elevations, and Krushelnycky et al. (2013) noted an increase in the number of zero rainfall days at a leeward high-elevation site on Maui. While it has been well established that rainfall patterns are influenced by phase changes in ENSO and PDO (e.g., Chu and Chen 2005; Frazier et al. 2012), recent evidence suggests rainfall patterns have decoupled from these modes in the last decade (Diaz and Giambelluca 2012). Results from this present analysis are in agreement with the notion of this decoupling and suggested that an alternative forcing mechanism may be responsible for the observed change.

Sustained increases in the TWI frequency pose several threats to high-elevation ecosystems including decreases in streamflow and groundwater recharge (Bassiouni and Oki 2013). Diaz et al. (2011) noted an increase in the lifting condensation level since about 2000 on the island of Hawaii, which combined with an increase in TWI frequency would reduce the thickness of the cloud zone thus decreasing rainfall and cloud water interception there (Giambelluca and Gerold 2011). In addition, the increases in TWI frequency over the past almost two decades may have already altered biota at high elevations. Increases in temperature, solar radiation, and the number of zero rainfall days, all of which are products of increased inversion frequency, have been linked to the decline of an iconic high-elevation endemic species, the Haleakalā Silversword, beginning in 1990 (Krushelnycky et al. 2013).

It is unclear if reported increases in TWI frequency and the subsequent decreases in rainfall will persist in the future. We have demonstrated that at least some of these trends can be linked to broader circulation patterns, potentially caused by anthropogenic global warming (Dai 2011). Lauer et al. (2013) has used future climate projections to determine that TWI frequency of occurrence will increase by 11%, and the TWI base height will decrease by ~160 m by 2100. If expected increases in the TWI frequency of occurrence

hold true additional decreases in high-elevation rainfall can be expected in both the dry and wet seasons in the future.

Acknowledgments. This work was partially supported by the U.S. Department of Interior Pacific Islands Climate Science Center (PICSC), the Hawaii Commission on Water Resource Management (CWRM), and the U.S. Army Corp of Engineers. Thanks to Larry D. Oolman for providing us with the atmospheric sounding data used in this analysis. We thank the staff of Haleakalā National Park Resource Management division and the Pacific Island Ecosystem Research Center (PIERC), USGS, for their long support of the HaleNet system. Special thanks to Lloyd Loope and Gordon Tribble of PIERC and to Mike Nullet, Camilo Mora, Abby Frazier, Paul Krushelnycky, and Ross Sutherland of the University of Hawai'i at Mānoa.

REFERENCES

Allen, R. J., J. R. Norris, and C. S. Zender, 2012: Recent Northern Hemisphere tropical expansion primarily driven by black carbon and tropospheric ozone. *Nature*, **485**, 350–354, doi:10.1038/nature11097.

Bassiouni, M., and D. S. Oki, 2013: Trends and shifts in streamflow in Hawai'i, 1913–2008. *Hydrol. Processes*, **27**, 1484–1500, doi:10.1002/hyp.9298.

Caballero, R., 2007: Role of eddies in the interannual variability of Hadley cell strength. *Geophys. Res. Lett.*, **34**, L22705, doi:10.1029/2007GL030971.

Cao, G. G., T. W. Giambelluca, D. E. Stevens, and T. A. Schroeder, 2007: Inversion variability in the Hawaiian trade wind regime. *J. Climate*, **20**, 1145–1160, doi:10.1175/JCLI4033.1.

Chikamoto, Y., and Coauthors, 2015: Skilful multi-year predictions of tropical trans-basin climate variability. *Nat. Commun.*, **6**, 6869, doi:10.1038/ncomms7869.

Chu, P. S., 1989: Hawaiian drought and the Southern Oscillation. *Int. J. Climatol.*, **9**, 619–631, doi:10.1002/joc.3370090606.

——, and H. Chen, 2005: Interannual and interdecadal rainfall variations in the Hawaiian Islands. *J. Climate*, **18**, 4796–4813, doi:10.1175/JCLI3578.1.

——, Y. R. Chen, and T. A. Schroeder, 2010: Changes in precipitation extremes in the Hawaiian Islands in a warming climate. *J. Climate*, **23**, 4881–4900, doi:10.1175/2010JCLI3484.1.

Compo, G. P., and Coauthors, 2011: The Twentieth Century Reanalysis project. *Quart. J. Roy. Meteor. Soc.*, **137**, 1–28, doi:10.1002/qj.776.

Crausbay, S. D., A. G. Frazier, T. W. Giambelluca, R. J. Longman, and S. C. Hotchkiss, 2014: Moisture status during a strong El Niño explains a tropical montane cloud forest's upper limit. *Oecologia*, **175**, 273–284, doi:10.1007/s00442-014-2888-8.

Dai, A., 2011: Drought under global warming: A review. *Wiley Interdiscip. Rev.: Climate Change*, **2**, 45–65, doi:10.1002/wcc.81.

Davis, S. M., and K. H. Rosenlof, 2012: A multidiagnostic intercomparison of tropical-width time series using reanalyses and satellite observations. *J. Climate*, **25**, 1061–1078, doi:10.1175/JCLI-D-11-00127.1.

Diaz, H. F., and T. W. Giambelluca, 2012: Changes in atmospheric circulation patterns associated with high and low rainfall regimes in the Hawaiian Islands region on multiple time scales. *Global Planet. Change*, **98–99**, 97–108, doi:10.1016/j.gloplacha.2012.08.011.

——, ——, and J. K. Eischeid, 2011: Changes in the vertical profiles of mean temperature and humidity in the Hawaiian Islands. *Global Planet. Change*, **77**, 21–25, doi:10.1016/j.gloplacha.2011.02.007.

Durbin, J., and G. S. Watson, 1971: Testing for serial correlation in least squares regression. III. *Biometrika*, **58**, 1–19.

Elison Timm, O., H. F. Diaz, T. W. Giambelluca, and M. Takahashi, 2011: Projection of changes in the frequency of heavy rain events over Hawaii based on leading Pacific climate modes. *J. Geophys. Res.*, **116**, D04109, doi:10.1029/2010JD014923.

Frazier, A. G., T. W. Giambelluca, and H. F. Diaz, 2012: Spatial rainfall patterns of ENSO and PDO in Hawai'i. *2012 Fall Meeting*, San Francisco, CA, Amer. Geophys. Union, Abstract B13B-0502.

——, ——, and ——, 2013: Mapping rainfall trends in Hawai'i. *2013 Fall Meeting*, San Francisco, CA, Amer. Geophys. Union, Abstract H43I-1580.

——, ——, ——, and H. L. Needham, 2015: Comparison of geostatistical approaches to spatially interpolate month-year rainfall for the Hawaiian Islands. *Int. J. Climatol.*, doi:10.1002/joc.4437, in press.

Giambelluca, T. W., 2005: Land use and water resources under a changing climate. *Encyclopedia of Hydrological Sciences*, M. G. Anderson and J. J. McDonnell, Eds., Vol. 5, John Wiley and Sons, 1–7.

——, and D. Nullet, 1991: Influence of the trade-wind inversion on the climate of a leeward mountain slope in Hawai'i. *Climate Res.*, **1**, 207–216, doi:10.3354/cr001207.

——, and T. A. Schroeder, 1998: Climate. *Atlas of Hawai'i*, 3rd ed. S. Juvik and J. Juvik, Eds., University of Hawai'i Press, 1–25.

——, and G. Gerold, 2011: Hydrology and biogeochemistry of tropical montane cloud forests. *Forest Hydrology and Biogeochemistry*, D. F. Levia, D. Carlyle-Moses, and T. Tanaka, Eds., Springer, 221–259.

——, H. F. Diaz, and M. S. A. Luke, 2008: Secular temperature changes in Hawai'i. *Geophys. Res. Lett.*, **35**, L12702, doi:10.1029/2008GL034377.

——, Q. Chen, A. G. Frazier, J. P. Price, Y.-L. Chen, P.-S. Chu, J. K. Eischeid, and D. M. Delparte, 2011: The rainfall atlas of Hawai'i. Final Rep., U.S. Army Corps of Engineers—Honolulu District and State of Hawai'i Commission on Water Resource Management, Honolulu, HI. [Available online at http://rainfall.geography.hawaii.edu.]

——, ——, ——, ——, ——, ——, ——, and ——, 2013: Online rainfall atlas of Hawai'i. *Bull. Amer. Meteor. Soc.*, **94**, 313–316, doi:10.1175/BAMS-D-11-00228.1.

Gotsch, S. G., S. D. Crausbay, T. W. Giambelluca, A. E. Weintraub, R. J. Longman, H. Asbjornsen, S. C. Hotchkiss, and T. E. Dawson, 2014: Water relations and microclimate around the upper limit of a cloud forest in Maui, Hawai'i. *Tree Physiol.*, **34**, 766–777, doi:10.1093/treephys/tpu050.

Grassi, B., G. Redaelli, P. O. Canziani, and G. Visconti, 2012: Effects of the PDO phase on the tropical belt width. *J. Climate*, **25**, 3282–3290, doi:10.1175/JCLI-D-11-00244.1.

Grindinger, C. M., 1992: Temporal variability of the trade wind inversion: Measured with a boundary layer vertical profiler.

M.S. thesis, Dept. of Meteorology, University of Hawai'i at Mānoa, 93 pp.

Hollander, M., and D. A. Wolfe, 1973: *Nonparametric Statistical Methods*. John Wiley and Sons, 503 pp.

Hu, Y., and Q. Fu, 2007: Observed poleward expansion of the Hadley circulation since 1979. *Atmos. Chem. Phys.*, **7**, 5229–5236, doi:10.5194/acp-7-5229-2007.

Kalnay, E., and Coauthors, 1996: The NCEP/NCAR 40-Year Reanalysis Project. *Bull. Amer. Meteor. Soc.*, **77**, 437–471, doi:10.1175/1520-0477(1996)077<0437:TNYRP>2.0.CO;2.

Kanamitsu, M., W. Ebisuzaki, J. Woollen, S. K. Yang, J. J. Hnilo, M. Fiorino, and G. L. Potter, 2002: NCEP–DOE AMIP-II Reanalysis (R-2). *Bull. Amer. Meteor. Soc.*, **83**, 1631–1643, doi:10.1175/BAMS-83-11-1631.

Kang, S. M., and J. Lu, 2012: Expansion of the Hadley cell under global warming: Winter versus summer. *J. Climate*, **25**, 8387–8393, doi:10.1175/JCLI-D-12-00323.1.

Killick, R., and I. Eckley, 2014: Changepoint: An R package for changepoint analysis. *J. Stat. Software*, **58**, 1–19.

Kitayama, K., and D. Mueller-Dombois, 1992: Vegetation of the wet windward slope of Haleakala, Maui, Hawaii. *Pac. Sci.*, **46**, 197–220.

Krushelnycky, P. D., L. L. Loope, T. W. Giambelluca, F. Starr, K. Starr, D. Drake, A. D. Taylor, and R. H. Robichaux, 2013: Climate-associated population declines reverse recovery and threaten future of an iconic high-elevation plant. *Global Change Biol.*, **19**, 911–922, doi:10.1111/gcb.12111.

Lauer, A., C. Zhang, O. Elison-Timm, Y. Wang, and K. Hamilton, 2013: Downscaling of climate change in the Hawaii region using CMIP5 results: On the choice of the forcing fields. *J. Climate*, **26**, 10 006–10 030, doi:10.1175/JCLI-D-13-00126.1.

Levinson, D. H., and M. C. Kruk, 2008: Evaluating the impacts of climate change on rainfall extremes for Hawaii and coastal Alaska. *24th Conf. on Severe Local Storms*, Savannah, GA, Amer. Meteor. Soc., 1.4. [Available online at https://ams.confex.com/ams/24SLS/techprogram/paper_142172.htm.]

Longman, R. J., 2015: The effects of trade wind inversion variability on high elevation climates in Hawai'i. Ph.D. dissertation, Department of Geography, University of Hawai'i at Mānoa, Honolulu, HI, 192 pp.

——, T. W. Giambelluca, R. J. Alliss, and M. L. Barnes, 2014: Temporal solar radiation change at high elevations in Hawai'i. *J. Geophys. Res. Atmos.*, **119**, 6022–6033, doi:10.1002/2013JD021322.

——, ——, M. A. Nullet, and L. L. Loope, 2015: Climatology of Haleakalā. University of Hawai'i Tech. Rep. 193, 126 pp.

Loope, L. L., and T. W. Giambelluca, 1998: Vulnerability of island tropical montane cloud forests to climate change, with special reference to east Maui, Hawaii. *Climatic Change*, **39**, 503–517, doi:10.1023/A:1005372118420.

Lu, J., G. A. Vecchi, and T. Reichler, 2007: Expansion of Hadley cell under global warming. *Geophys. Res. Lett.*, **34**, L06805, doi:10.1029/2006GL028443.

Lucas, C., B. Timbal, and H. Nguyen, 2014: The expanding tropics: A critical assessment of the observational and modeling studies. *Wiley Interdiscip. Rev.: Climate Change*, **5**, 89–112, doi:10.1002/wcc.251.

Lyons, S. W., 1982: Empirical orthogonal function analysis of Hawaiian rainfall. *J. Appl. Meteor.*, **21**, 1713–1729, doi:10.1175/1520-0450(1982)021<1713:EOFAOH>2.0.CO;2.

McGregor, S., A. Timmermann, M. F. Stuecker, M. H. England, M. Merrifield, F. F. Jin, and Y. Chikamoto, 2014: Recent Walker circulation strengthening and Pacific cooling amplified by Atlantic warming. *Nat. Climate Change*, **4**, 888–892, doi:10.1038/nclimate2330.

Merrifield, M. A., 2011: A shift in western tropical Pacific sea level trends during the 1990s. *J. Climate*, **24**, 4126–4138, doi:10.1175/2011JCLI3932.1.

Mitas, C. M., and A. Clement, 2005: Has the Hadley cell been strengthening in recent decades? *Geophys. Res. Lett.*, **32**, L03809, doi:10.1029/2004GL021765.

——, and ——, 2006: Recent behavior of the Hadley cell and tropical thermodynamics in climate models and reanalyses. *Geophys. Res. Lett.*, **33**, L01810, doi:10.1029/2005GL024406.

Nguyen, H., A. Evans, C. Lucas, I. Smith, and B. Timbal, 2013: The Hadley circulation in reanalyses: Climatology, variability, and change. *J. Climate*, **26**, 3357–3376, doi:10.1175/JCLI-D-12-00224.1.

Oort, A. H., and J. J. Yienger, 1996: Observed interannual variability in the Hadley circulation and its connection to ENSO. *J. Climate*, **9**, 2751–2767, doi:10.1175/1520-0442(1996)009<2751:OIVITH>2.0.CO;2.

Polvani, L. M., D. W. Waugh, G. J. P. Correa, and S.-W. Son, 2011: Stratospheric ozone depletion: The main driver of twentieth-century atmospheric circulation changes in the Southern Hemisphere. *J. Climate*, **24**, 795–812, doi:10.1175/2010JCLI3772.1.

Quan, X.-W., H. F. Diaz, and M. P. Hoerling, 2004: Change in the tropical Hadley cell since 1950. *The Hadley Circulation: Past, Present and Future*, H. F. Diaz and R. S. Bradley, Eds., Kluwer Academic, 85–120.

——, M. P. Hoerling, J. Perlwitz, H. F. Diaz, and T. Xu, 2014: How fast are the tropics expanding? *J. Climate*, **27**, 1999–2013, doi:10.1175/JCLI-D-13-00287.1.

Riehl, H., 1979: *Climate and Weather in the Tropics.* Academic Press, 623 pp.

Seidel, D. J., Q. Fu, W. J. Randel, and T. J. Reichler, 2008: Widening of the tropical belt in a changing climate. *Nat. Geosci.*, **1**, 21–24, doi:10.1038/ngeo.2007.38.

Shapiro, S. S., and M. B. Wilk, 1965: An analysis of variance test for normality (complete samples). *Biometrika*, **52**, 591–611, doi:10.1093/biomet/52.3-4.591.

Sohn, B. J., and S. C. Park, 2010: Strengthened tropical circulations in past three decades inferred from water vapor transport. *J. Geophys. Res.*, **115**, D15112, doi:10.1029/2009JD013713.

Song, H., and M. Zhang, 2007: Changes of the boreal winter Hadley circulation in the NCEP–NCAR and ECMWF reanalyses: A comparative study. *J. Climate*, **20**, 5191–5200, doi:10.1175/JCLI4260.1.

Stachnik, J. P., and C. Schumacher, 2011: A comparison of the Hadley circulation in modern reanalyses. *J. Geophys. Res.*, **116**, D22102, doi:10.1029/2011JD016677.

Staten, P. W., J. J. Rutz, T. Reichler, and J. Lu, 2012: Breaking down the tropospheric circulation response by forcing. *Climate Dyn.*, **39**, 2361–2375, doi:10.1007/s00382-011-1267-y.

Tanaka, H. L., N. Ishizaki, and A. Kitoh, 2004: Trend and interannual variability of Walker, monsoon and Hadley circulations defined by velocity potential in the upper troposphere. *Tellus*, **56A**, 250–269, doi:10.1111/j.1600-0870.2004.00049.x.

Thorne, P. W., and R. S. Vose, 2010: Reanalyses suitable for characterizing long-term trends: Are they really achievable? *Bull. Amer. Meteor. Soc.*, **91**, 353–361, doi:10.1175/2009BAMS2858.1.

Timm, O., and H. F. Diaz, 2009: Synoptic-statistical approach to regional downscaling of IPCC twenty-first-century climate projections: Seasonal rainfall over the Hawaiian Islands. *J. Climate*, **22**, 4261–4280, doi:10.1175/2009JCLI2833.1.

Tran, L. T., 1995: Relationship between the inversion and rainfall on the island of Maui. M.A. thesis, University of Hawai'i at Mānoa, Honolulu, HI, 115 pp.

Trenberth, K. E., D. P. Stepaniak, and J. M. Caron, 2000: The global monsoon as seen through the divergent atmospheric circulation. *J. Climate*, **13**, 3969–3993, doi:10.1175/1520-0442(2000)013<3969:TGMAST>2.0.CO;2.

Uppala, S. M., and Coauthors, 2005: The ERA-40 Re-Analysis. *Quart. J. Roy. Meteor. Soc.*, **131**, 2961–3012, doi:10.1256/qj.04.176.

Wang, C., 2002: Atmospheric circulation cells associated with the El Niño–Southern Oscillation. *J. Climate*, **15**, 399–419, doi:10.1175/1520-0442(2002)015<0399:ACCAWT>2.0.CO;2.

Wolter, K., and M. S. Timlin, 1998: Measuring the strength of ENSO events: How does 1997/98 rank? *Weather*, **53**, 315–324, doi:10.1002/j.1477-8696.1998.tb06408.x.

Yin, J. H., 2005: A consistent poleward shift of the storm tracks in simulations of 21st century climate. *Geophys. Res. Lett.*, **32**, L18701, doi:10.1029/2005GL023684.

Yu, J.-Y., P.-K. Kao, H. Paek, H.-H. Hsu, C.-W. Hung, M.-M. Lu, and S.-I. An, 2015: Linking emergence of the central Pacific El Niño to the Atlantic multidecadal oscillation. *J. Climate*, **28**, 651–662, doi:10.1175/JCLI-D-14-00347.1.